https://dx.doi.org/10.4314/ijs.v28i2.2
Ife Journal of Science vol. 28, no. 2 (2026)

NEURAL ORDINARY DIFFERENTIAL EQUATIONS FOR PARAMETER ESTIMATION, SIMULATION AND FORECASTING OF INFECTIOUS DISEASE DYNAMICS: APPLICATIONS TO HIV/AIDS AND MALARIA MODELS

Ndubuogaranya, F. C., Ehigie, J. O.* and Okunuga, S. A.
Department of Mathematics, University of Lagos, Lagos, Nigeria.
Ndubuogaranya F.C. https://orcid.org/0009-0004-6773-7012; Ehigie J.O. https://orcid.org/0000-0002-3159-5743;
Okunuga S.A. https://orcid.org/0000-0003-4139-8441
*Corresponding Author's Email: jehigie@unilag.edu.ng
(Received: 3rd March, 2026; Accepted: 15th July, 2026)

ABSTRACT

This study investigates the application of Neural Ordinary Differential Equations (Neural ODEs) for the simulation and parameter estimation of disease models. The primary objective is to simulate disease dynamics and forecast future transmission trends using a trained Neural ODE framework. The model adopts a numerically informed and data-driven approach that integrates epidemiological datasets with disease-informed neural networks to capture transmission behaviour. For HIV/AIDS, transmission dynamics are generated using synthetic datasets obtained via the fourth-order Runge-Kutta method, whereas predictions for malaria are based on real-world epidemiological data. The results demonstrate that the Neural ODE framework effectively learns disease transmission patterns, accurately captures the progression of compartmental dynamics, estimates key epidemiological parameters, and produces reliable forecasts from both observed and numerically generated data. It is observed that increasing the number of training epochs improves predictive performance, as the model better captures complex nonlinear patterns and fluctuations within disease compartments. However, a notable limitation is that higher epoch counts substantially increase computational time, with training durations extending to several hours.

Keywords: Neural ODEs, Neural Network, Epidemiology, Compartmental Model, Runge Kutta Method.

INTRODUCTION

Infectious diseases have always been a major threat to human and global public health, often leading to death and mortality while significantly impacting social and economic stability. In Africa, humans have had to suffer from so many severe infectious diseases such as malaria, Lassa fever, HIV/AIDS, tuberculosis, influenza, Ebola, measles and most recently COVID-19. As a result of these diseases outbreaks, several strategies have been developed to understand transmission mechanisms and improve prevention and controls of these infectious diseases. Among the strategies, mathematical epidemiology emerged as a powerful analytical framework for quantifying disease dynamics and understanding the effect of parameters influencing the spread of diseases and informing effective public-health interventions.

Mathematical modelling of infectious disease generally adopts either stochastic or deterministic approaches. For instance, the deterministic model divides the population into different compartments such as Susceptible (S), Infectious (I), and Recovered (R), thereby determining the rate of transition between these compartments.

Dynamic models play a very important role in simulating real life situation. It helps in the analysis, simulation and prediction of complex systems across sciences and other fields. Traditionally, dynamic systems are modelled as an ordinary differential equation (ODEs) and solved using numerical methods. However, since the technological advancement of computational science and machine learning algorithms, data-driven modelling has emerged as a promising framework for learning continuous-time dynamics. Neural ODEs method has shown great promise in modelling and capturing the behaviour of dynamic system directly from data while preserving the interpretability of differential equation models.

In infectious disease modelling, the numerical simulation of the dynamics of infectious diseases models are mostly computed using numerical methods such as the Runge-Kutta method (Asri *et al.* (2021), Wang *et al.* (2016)) and often rely on statistical parameters obtained from existing studies and literature. This approach introduces uncertainty in the results of the actual dynamics, progression trends, and spread of disease populations. To overcome the shortcomings, the present study explores the application of Neural ODEs to selected disease using a neural ODEs

approach to learn directly from empirical data. This approach aims to enhance predictive accuracy and improve reliability of forecasts derived from graphical visualization.

Another major challenge is the problem of choosing a suitable numerical method, particularly when real-world data are scarce or unavailable. In such cases, numerical methods will be responsible for generating synthetic datasets which will be used in training the neural network model and the overall performance of the neural ODE models to accurately predict solutions of the dynamic systems. The classical fourth-order Runge-Kutta (RK4) method known for its order of accuracy and stability, is therefore adopted in this research as the primary numerical integration scheme supporting the Neural ODE framework.

This research applies the developed Neural ODE methodology to two infectious disease models: an HIV/AIDS transmission model and a malaria compartmental model, demonstrating its flexibility in modelling different diseases with differing transmission characteristics and epidemiological dynamics. Such flexibility is especially important for responding effectively to emerging and re-emerging infectious threats, where rapid and accurate modelling is essential for timely intervention planning. Consequently, Neural ODEs provide a versatile modelling framework capable of accommodating diverse epidemiological scenarios.

Mathematical modelling of disease has been an indispensable tool in accounting for disease transmission dynamics as well as disease spread (Kamina *et al.*, 2019). Historically, infectious diseases modelling has long relied on compartmental (deterministic) models. The most basic compartmental model is the Susceptible-Infected-Recovered (SIR) model, a method developed by Kermack and McKendrick (1927) in the paper "*A contribution to the Mathematical Theory of Epidemics*". The SIR model is capable of generating realistic single-epidemic outbreaks and also provided important theoretical epidemiological insights and predicts depending on the transmission potential of the infection and the critical fraction of susceptible in the population that must be exceeded if an epidemic is to occur (Choisy *et al.*, 2006, Shaier *et al.*, 2022).

Extensions of the classical SIR model have been developed to address specific epidemiological contexts. For example, Zakary *et al.* (2016) proposed the SIR model for studying the impact of awareness programs on HIV/AIDS transmission by incorporating behavioural modifications that reduce susceptibility. To ensure there is an accurate modelling of the disease transmission, it requires high-quality data on the vectors populations (necessary if the disease to be studied is a vector-borne disease), human infection rates, and environmental conditions. The classical SIR model was extended to the $SEIR$ model where the Exposed (E) compartment was added to it, which was introduced by Aron *et al.* (1984), to account for those who have been infected but are not yet infectious. The Exposed compartment introduced in the $SEIR$ model is effective for the modelling of malaria, as it accounts for the population of individuals that are infected by the Plasmodium parasites, but not capable of passing on the infection to others during a latent period Mandal. This latent period is essential in malaria dynamics due to the time it takes for the parasite to develop within the human host and the mosquito vector. Turner *et al.* (2015)) studied the spread of malaria in humans and mosquitoes, using the $SEIR$ model for the human population and the Susceptible, Exposed and Infected (SEI) model for the mosquitoes' population. From their findings, they concluded that the combination of the $SEIR$ and SEI models were used to show the growth and spread of malaria, allowing for a detailed analysis and prediction of the interactions between humans and vectors that contributes to the spread of malaria.

Numerical solution techniques such as Runge Kutta (RK) Method have been widely used as the numerical approach for solving ordinary differential equations that arises in the modelling of the spread of infectious diseases. This method has a smaller rounding error and is known for having a high level of precision that can meet most precision requirements, and the computational complexity can also meet the performance requirements of most processors Yion (2023). For example, Simangunsong and Mungkasi (2021) applied the fourth-order Runge Kutta (RK4) method to the Susceptible-Infected-AIDs (SIA) model for the behaviour and prediction of the spread of HIV/AIDs transmission. Their results

demonstrated that the RK4 provides a numerical solution for the HIV/AIDs transmission model effectively and based on the numerical solutions, in a longer time, the susceptible, infected, AIDs cases and total population will each reach their equilibrium points.

Neural ODEs extend the capability of traditional ODE models by parameterizing the derivative of the hidden state using a neural network (Chen *et al.*, 2018). This allows for learning complex dynamics directly from data. Applying Neural ODEs to the SIR model involves replacing the fixed ODE system with a neural network that learns the underlying dynamics of disease transmission:

$$\frac{dy(t)}{dt} = f(y(t), t, \theta) \quad (1)$$

This approach allows the model to adapt to varying disease dynamics and external factors, improving prediction accuracy.

Recent developments have further integrated epidemiological modelling with machine learning frameworks. For instance, Rodríguez et al. (2023) introduced Epidemiologically-Informed Neural Networks (EINNs), which combine mechanistic epidemic models with physics-informed neural networks (PINNs) to capture latent epidemic dynamics and enhance long-term forecasting accuracy. They leveraged on the selective superiorities of both machine learning models and epidemiological ODEs (SIR) models to have predictions that are accurate and well-correlated with even longer-term epidemic trends. Similarly, Shaier *et al.* (2022) developed a Disease-Informed Neural Network (DINN), integrating classical SIR models with PINN methodologies to effectively predict the dynamics of the spread of various infectious disease and demonstrated how the neural networks are capable of learning the diseases spread, forecasting their progression, and finding their unique parameters. Additionally, Kosma *et al.* (2023) presented a computational approach to model the contagion dynamics underlying infectious diseases focusing on the SIR epidemic model on neural networks, demonstrating strong predictive performance for epidemic evolution on complex networks.

Furthermore, Millevoi *et al.* (2024) proposed a Physics-Informed Neural Network (PINN) framework for compartmental epidemiological models to estimate time-varying transmission rates and state variables during disease outbreaks. Their reduced-split training strategy improved prediction accuracy and computational efficiency, demonstrating the effectiveness of PINNs for parameter estimation and short-term epidemic forecasting. Similarly, Han *et al.* (2024) developed a PINN model embedded within the classical SIR framework to investigate the temporal dynamics of infectious diseases. Using both synthetic and real COVID-19 datasets, they demonstrated that PINNs can accurately capture disease transmission trends and provide reliable epidemic forecasts even when simplified epidemiological models are employed. In a comprehensive review, Liu *et al.* (2024) examined the application of Graph Neural Networks (GNNs) in epidemic modelling and forecasting. Their study highlighted the ability of GNNs to capture complex spatial and temporal transmission patterns while identifying future research opportunities for integrating epidemiological knowledge with graph-based learning frameworks. Extending the application of Neural ODEs in epidemiology, Wan *et al.* (2024) introduced the Epidemiology-Aware Neural ODE with Continuous Disease Transmission Graph (EARTH) framework for epidemic forecasting. By combining Neural ODEs with disease transmission graphs, the model effectively learned regional transmission dynamics and achieved superior forecasting performance compared to existing approaches. More recently, Sharma *et al.* (2026) reviewed the growing role of Artificial Intelligence in epidemic modelling and pandemic preparedness. Their study highlighted the contributions of machine learning, deep learning, graph neural networks, and hybrid epidemiological models in disease forecasting, parameter estimation, surveillance, and public health decision-making.

MATERIALS AND METHODS

Neural Ordinary Differential Equations

The Neural ODEs framework adopts a data driven and numerically informed approach to predict disease transmission dynamics through the combination of epidemiological data with a disease-informed neural network. In this research, the methodology is generalized to two prevalent diseases using epidemiological compartmental structures derived from the classical SIR model as a base case for the architecture. This section

outlines the framework for the numerical computation (Shaier *et al.*, 2022).

Compartmental Model

Consider the SIR model used to model the disease transmission within a population over time, defined by the following ordinary differential equations:

$$\frac{dS}{dt} = -\beta \frac{S(t)I(t)}{N}$$
$$\frac{dI}{dt} = \beta \frac{S(t)I(t)}{N} - \gamma I(t) \quad (2)$$
$$\frac{dR}{dt} = \gamma I(t)$$

where:

$S(t)$ represents the number of susceptible individuals at time t,

$I(t)$ represents the number of infected individuals at time t,

$R(t)$ represents the number of recovered individuals at time t,

β represents the transmission rate,

γ represents the recovery rate,

N represents the total population, $N = S(t) + I(t) + R(t)$.

To generate synthetic data for diseases where real life data are unavailable, the systems of ordinary differential equations that defines the SIR model in Equation *SIR* is solved numerically using the classical fourth-order Runge-Kutta method (RK4) based on the defined transmission rate β and recovery rate γ. The RK4 method is best known for its higher accuracy, versatility and computational efficiency. In this research, the RK4 algorithm is implemented explicitly in Python to approximate the solution of the SIR model by calculating weighted averages of derivatives at discrete time steps.

The one-step computation of the classical fourth-order Runge-Kutta method is implemented as follows:

$$k_1 = f(x_n, y_n)$$
$$k_2 = f\left(x_n + \frac{h}{2}, y_n + \frac{hk_1}{2}\right)$$
$$k_3 = f\left(x_n + \frac{h}{2}, y_n + \frac{hk_2}{2}\right)$$
$$k_4 = f\left(x_n + h, y_n + hk_3\right)$$

Then the next step value is computed as:

$$y_{n+1} = y_n + \frac{h}{6}(k_1 + 2(k_2 + k_3) + k_4) \quad (3)$$

Architecture of the Neural Network

A neural network is a deep learning architecture inspired by the structure and functioning of the human brain. In this research, the Neural ODEs model, which embeds the neural network within the differential equation formulation, is used. This technique gives us the leverage to learn complex disease dynamics from data while retaining the interpretability of the dynamical systems. In particular, Neural ODEs model the derivative of the hidden state using neural networks which can be mathematically expressed as:

$$\frac{dy}{dt} = f(y(t), t, \theta) \quad (4)$$

Where $y(t) = [S(t), I(t), R(t)]$ represents the state vector, representing the susceptible, infected, and recovered populations, respectively and $f(y(t), t, \theta)$ is a neural network parameterized by θ, which includes the learnable parameters β and γ.

The neural network is therefore used to model the transmission dynamics of the *SIR* model. It predicts the temporal evolution of the compartments S, I and R and also learn the system's parameters β and γ, which defines the spread and control of the disease. The adopted architecture is designed as a fully connected feedforward network, with the time steps as inputs and S, I and R as outputs. The fully connected network is organized into layers of neurons where each neuron in one layer is connected to every neuron in the subsequent layer (except for the output layer), and each connection assigned a particular weight (Shaier *et al.*, 2022).

Figure 1 illustrates the diagram of the neural network architecture for the *SIR* model. The structure comprises the flow from three input layer, through eight hidden layers, each containing 20 neurons, that process the input data using activation functions to capture complex behaviour between compartments, to the output layer, which provides predicted for new values of S, I, R based on the learned system parameters.

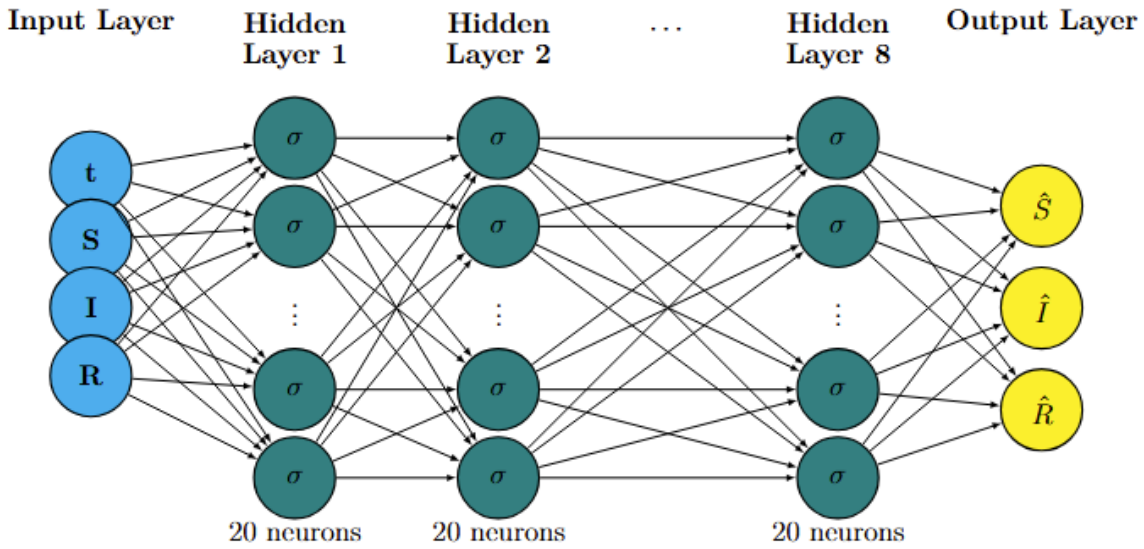

Figure 1: A simple Neural Network Architecture for the S, I, R model

Computational Environment

All simulations and model training were conducted using Python *"3.12.13"* within a Jupyter Notebook environment with a random seeds of *'1234'*. The neural network models were implemented using PyTorch *"2.11.0+cpu"*. Experiments were conducted on Google Colab using the default CPU (Intel Core i7, 16GB RAM) runtime (Intel (R) Xeon (R) CPU @ 2.20GHz, 12.7GB RAM and 107.7GB Disk), running on Windows 11 Pro operating system. Additional libraries utilized in this study included NumPy, Pandas, Matplotlib, and SciPy for data processing, visualization, and numerical computations.

Define the Neural Network

The neural network is defined as a class, named Diseased-Informed Neural Network *DINN*, which is used to simulate the dynamics of the model by estimating unknown system parameters from previously acquired real-world data.

A multilayer feedforward neural network architecture with will be used, which consists of:
Input Layer: The input to the neural network is a batch of time steps t, then, *DINN* class receives the time vector t and the corresponding (S, I, R) data.

Hidden Layer. The connected hidden layers together with the number of neurons will be specified. The activation function used at each layer is the ReLU (Rectified Linear Unit), which introduces non-linearity into the model and helps it learn complex behaviour between the time steps and the dynamics of the disease transmission.

Output Layer. The output to the neural network has 3 neurons corresponding to the predicted values of the three compartments of the disease model (S, I, R) for each time step. Mathematically, the neural network output is computed as:

$$\sigma\left(\sum_{i=1}^{n} x_i w_i + b\right) \rightarrow \text{Output}$$

where:

n represents the number of incoming connections,

x_i represents the value of each incoming neuron of the i th layer,

w_i represents the weight on each connection of the i th layer,

b represents the bias term, and

σ represents the activation function.

Normalization

Normalization is applied to the S, I and R compartments to ensure that the S, I and R compartment values fed into the neural network remain within the same range of [0, 1] which is suitable for neural network training. This procedure prevents the susceptible compartment, which is much larger, from dominating the training process and thereby improves numerical stability and convergence.

The normalization is performed using the standard min-max scaling:

$$\hat{X} = \frac{X - X_{\min}}{X_{\max} - X_{\min}} \quad (5)$$

where $\hat{X}$ is the normalized value representing each compartments, $\hat{S}$, $\hat{I}$ or $\hat{R}$; X is the original value representing each compartments, $X_{\min}$ is the minimum values of each compartments and $X_{\max}$ is the maximum values of each compartments.

This scaling ensures balanced training and enhances the robustness of the neural network's parameter estimation.

Optimizing the Neural Network

The neural network is optimized to learn the underlying dynamics of the disease dynamics and to predict the normalized compartments $(\hat{S}, \hat{I}, \hat{R})$. Next, we compute gradients of each normalized compartment with respect to time using automatic differentiation. This is achieved through backpropagating within the network, allowing the integration of the learned derivatives of the normalized compartments to be incorporated consistently into the *SIR* ODEs.

Mathematically, this is expressed as:

$$\frac{d\hat{X}(t)}{dt} = \nabla_t(\hat{X}(t)) \quad (6)$$

where $\nabla_t(\hat{X}(t))$ represents the gradient of each compartments $\hat{S}$, $\hat{I}$ or $\hat{R}$, with respect to time t.

After training, the predicted normalized compartments values are transformed to the original scale. The inverse normalization is given by

$$X = X_{\min} + (X_{\max} - X_{\min}) + \hat{X} \quad (7)$$

where X represents the original compartment values S, I and R.

To assess the consistency of the neural network with the epidemiological model, the residuals of each compartment of the *SIR* model are calculated, which quantifies the difference between the predicted derivatives of the normalized compartments from the neural network and the corresponding *SIR* ODEs. They therefore measure the performance of the neural network predictions and how well it aligns with the governing dynamical model. The residuals are defined as

$$\hat{f}_1(t) = \frac{\frac{d\hat{S}}{dt} - \left(-\frac{\beta}{N}S(t)I(t)\right)}{S_{\max} - S_{\min}}$$

$$\hat{f}_2(t) = \frac{\frac{d\hat{I}}{dt} - \left(\frac{\beta}{N}S(t)I(t) - \gamma I(t)\right)}{I_{\max} - I_{\min}} \quad (8)$$

$$\hat{f}_3(t) = \frac{\frac{d\hat{R}}{dt} - \gamma I(t)}{R_{\max} - R_{\min}}$$

where $\hat{f}_1(t)$, $\hat{f}_2(t)$ and $\hat{f}_3(t)$ represents the residuals of each compartment, respectively.

Training the Neural Network

The training process for Neural ODEs involves optimizing the neural network parameters to minimize the difference between the model's predicted states as learned by the neural network and the actual states given by the *SIR* system of ODES over a given time. The principal components of the training procedure are outlined below.

Loss Function: A loss function is defined to quantify the discrepancy between the predicted *SIR* model and the actual *SIR* data. To implement this, the Mean Squared Error (MSE) is employed to measure this difference for each compartment of the *SIR* model and the predicted states. The MSE is also applied to the residuals of each compartment for the *SIR* model. Thus, the total MSE is calculated mathematically as:

$$MSE = MSE_{sir} + MISE_f \text{ M}$$

where

$$MSE_{sir} = \frac{1}{N_{sir}}\left[\sum_{i=1}^{N_{sir}} |\, \hat{y}(t_i) - y(t_i)\,|^2\right]$$

and

$$MSE_f = \frac{1}{N_f}\left[\sum_{i=1}^{N_f} |\, f_i\,|^2\right]$$

Consequently, the overall loss function is expressed as:

$$Loss = MSE(S_{act} - S_{pre}) + MSE(I_{act} - I_{pre}) + MSE(R_{act} - R_{pre}) + MSE(f_1) + MSE(f_2) + MSE(f_3) \quad (9)$$

Here, S_{act}, I_{act} and R_{act} denote observed epidemiological data, S_{pre}, I_{pre} and R_{pre}

represent the neural network predictions, N_{sir} and N_f are the number of time steps (data points) for the data and residuals respectively, $\hat{y}(t_i)$ and $y(t_i)$ denote predicted and observed states, and f_i are the residuals.

Optimizer. An optimizer algorithm is necessary for updating the network weights, biases and the learnable parameters (β and γ) of the neural network to minimize the loss function. In this research, the *Adam optimizer* is adopted due to its efficiency and robustness, which updates the parameters θ of the neural network iteratively during training using the computed gradients, thereby, minimizing the loss function. The update rule using the gradient descent is expressed as:

$$\theta_{i,t+1} = \theta_{i,t} - \eta \nabla_\theta L(\theta) \qquad (10)$$

where η is the learning rate, $\theta_{i,t+1}$ represents the new value of the neural network's parameters, and $\theta_{i,j}$ represents the old value of the neural network's parameters.

Gradient Computation: The gradient of the loss function with respect to the parameters of the neural network is computed using backpropagation. This process involves backpropagating through the neural network for each predicted compartments of the *SIR* model. Thus, the gradient of the loss function is expressed as

$$\nabla_\theta L(\theta) = \frac{\partial L(\theta)}{\partial \hat{y}(t_i)} \cdot \frac{\partial \hat{y}(t_i)}{\partial \theta} \qquad (11)$$

where θ denotes the set of trainable parameters and $\nabla_\theta L(\theta)$ represents the gradient of the loss function.

Relative Error. To further evaluate predictive performance, the relative error is calculated for each compartment. This provides a normalized measure of the discrepancy between predicted and actual data. It is defined as

$$y_{error} = \sqrt{\frac{\sum_{t=1}^{T} \left(y(t_i) - \hat{y}(t_i)\right)^2}{\sum_{t=1}^{T} \left(y(t_i)\right)^2}} \qquad (12)$$

Here, $\hat{y}(t_i)$ and $y(t_i)$ are the predicted values and actual compartment values, respectively for each compartment of the *SIR* model respectively.

Parameter Estimation

The Neural ODEs model applies a data driven and numerically informed approach to estimate the parameters of the diseases model. The neural network learns the rate of transmission and recovery of the disease model from real-world and generated data which shows how the disease is spread over time.

In this research, we utilize a disease-informed neural network by incorporating the SIR ODEs into the neural network, without any prior knowledge of the transmission and recovery parameters. Parameter estimation occurs during the training and the optimization process of the neural network. In the python codes, the parameters, β and γ are printed after every 1000 epochs, which allows us to track the progress of the training ensuring the values of β and γ are changing as the model is training over time. These feedback helps us monitor if the model is converging towards reasonable parameter values for the transmission and recovery rate.

As the neural network iteratively updates its parameters, the code outputs the current estimate of the disease model's parameter. For the generated data, the actual parameters of the disease model are provided from literature, but the training of the neural network is done without it because it will learn the parameters from the generated data points.

To assess the accuracy of the parameter estimation, the relative error in percentage is calculated for each parameter, which quantifies the error between the estimated parameters and the actual parameters. The % Relative Error is defined as

$$\%Error = \frac{Actual\ Parameter - Estimated\ Parameter}{Actual\ Parameter} \times 100\% \qquad (13)$$

RESULTS AND DISCUSSION

Numerical Simulation

In this section, Neural ODE is applied to estimate the parameters, simulate and predict the spread of HIV/AIDs and malaria using existing models as the base cases for exploring the Neural ODE framework. For HIV/AIDS, transmission dynamics are generated using synthetic datasets obtained via the fourth-order Runge-Kutta method, whereas predictions for malaria are based on real-world epidemiological data. This is achieved by fitting the Neural ODEs model to each disease, followed by a discussion of the corresponding results.

Numerically Informed Approach: HIV/AIDs

Consider a model to describe the dynamics of HIV/AIDs spread presented in Kibona *et al.* (2011). The model is divided into four compartments: Susceptible, Infected, Pre AIDs Patients and AIDs Patients ($SIPA$). The susceptible (S) individual become infected through sexual contact with infected (I) individuals, which may lead to the birth of infected children who either the infected stage immediately or dies at birth. Once infected, some individual may move to the pre-AIDs (P) stage, depending on the viral load, while some with serious infection moves directly to the AIDs (A) stage. Both pre-AIDs patients and AIDs patient are assumed to be sexually inactive and thus not infectious. Table 1 summarizes the parameters of the SIPA model and Figure 2 illustrates the interaction between the compartments.

Table 1: Description of the parameters of the HIV/AIDs model

Parameter	Description
Q	Recruitment rate of susceptible individuals into the population
ν	Natural mortality rate
α	Disease-induced death rate
β	Sexual contact rate
c	Number of partners per individual
μ	Rate of movement of pre-AIDS stage individuals into AIDS stage
$(1-\varepsilon)\theta$	Rate of recruitment of infected newborn into the infected class
$\alpha\delta$	Rate at which infected individuals move into the pre-AIDs stage
$m\pi I$	Recruitment of pre-AIDs immigrant into the population
$m(1-\pi)I$	Recruitment of infected immigrants into the population
$(1-\sigma)\delta$	Rate at which infected individuals move into the AIDs stage
N	Total population: $N = S + I + P + A$

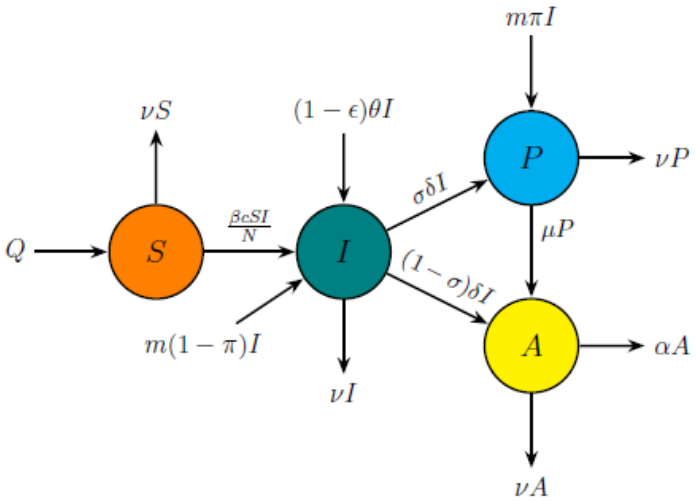

Figure 2: Flow Diagram of the HIV/AIDs model

Kibona *et al.* (2011) formulated the following systems of ODEs which describes the dynamics of the spread of HIV/AIDs.

$$\frac{dS}{dt} = Q - \frac{\beta}{N} cSI - \nu S$$

$$\frac{dI}{dt} = m(1-\pi)I + \frac{\beta}{N} cSI - (\delta + \nu)I + (1-\varepsilon)\theta I \quad (14)$$

$$\frac{dP}{dt} = (m\pi + \sigma\delta)I - (\mu + \nu)P$$

$$\frac{dA}{dt} = (1-\sigma)\delta I + \mu P - (\alpha + \nu)A$$

For numerical simulation of (14), 200 data points (from year 1 to year 35) were generated for the SIPA model using known parameters in Kibona *et al.* (2011), by solving the *SIPA* ODEs with classical Runge-Kutta method. The neural network employed for the *SIPA* model comprises 8 fully connected hidden layers, which consists of 20 neurons each. With a learning rate of 1×10^{-5}, the model was trained for 100,000 epochs (approximately 18 mins 56 secs). The relative error corresponding to the four compartments of the HIV/AIDs model over time are $S_{error} = 8.26529\times10^{-3}$, $I_{error} = 2.56014\times10^{-3}$, $P_{error} = 2.73932\times10^{-3}$, $A_{error} = 2.19732\times10^{-3}$. The trained neural network estimates the learnable parameters Q, ν, c, α, β, ε, θ, μ, m, π, δ, and σ. Figure 3 and Table 2 present the time evolution of the compartments and estimated parameters, respectively. We calculate the relative error in percentage for the estimated parameters, to show the error between the actual and the obtained parameters from the training.

Table 2: Parameter Estimation - HIV/AIDs

Parameter	Actual Value	Range	Estimated Parameter	Relative Error (%)
Q	2000	(1995, 2005)	2000.448731	0.022437
ν	0.014286	(0.01, 0.02)	0.014803	3.623104
c	25	(24, 26)	25.040854	0.163414
α	1.00	(0, 2)	1.000940	0.094032
β	0.05	(0.049, 0.051)	0.049843	0.313802
ε	0.40	(0.39, 0.41)	0.404458	1.114608
θ	0.01	(0.0099,0.011)	0.010276	2.760001
μ	0.50	(0.49, 0.51)	0.506695	1.338995
m	0.01	(0.0099, 0.011)	0.010440	4.403766
π	0.30	(0.29, 0.31)	0.296216	1.261439
δ	0.20	(0.19, 0.21)	0.200266	0.133151
σ	1.00	(0, 2)	1.011446	1.144576

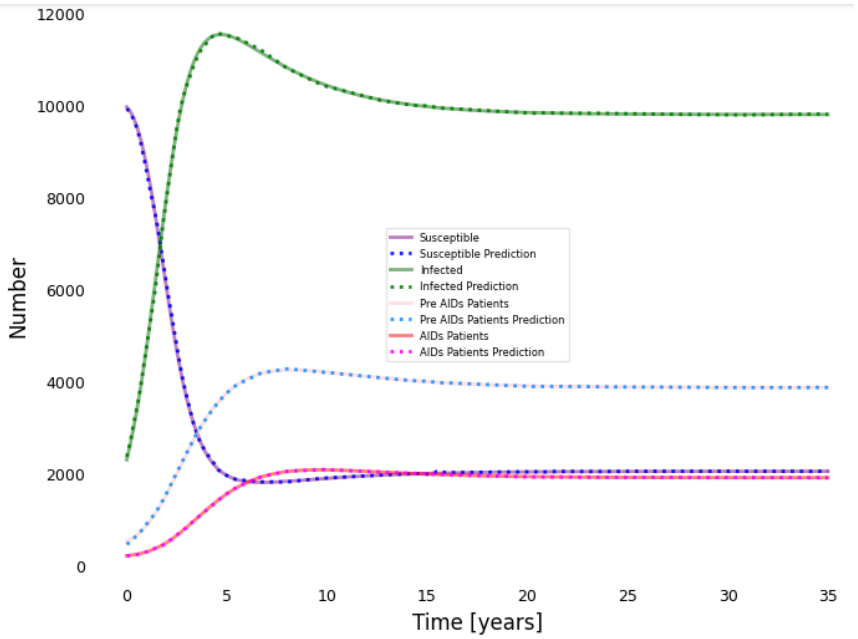

Figure 3: Time evolution of Actual vs Predicted for HIV/AIDs

Global Sensitivity Analysis (PRCC)

A global sensitivity analysis was performed using Latin Hypercube Sampling with time-dependent partial rank correlation coefficients (PRCC) for the infected (I), pre-AIDS (P), and AIDS (A) compartments. The PRCC plot is shown in Figure 4, and the temporal evolution of each parameter's influence in Figure 5.

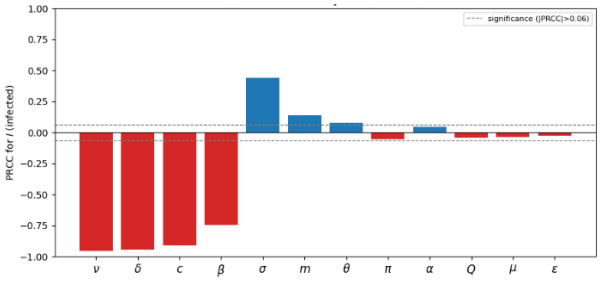

(a) PRCC – Infected Human

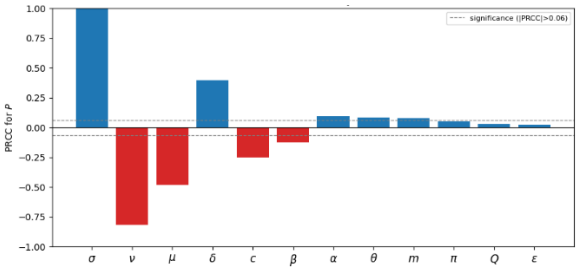

(b) PRCC – Pre-AIDS Patient

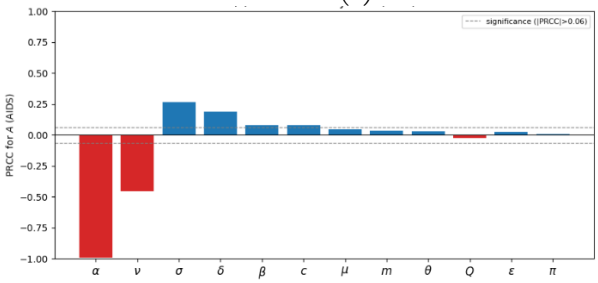

(c) PRCC – AIDS Patient

Figure 4: Sensitivity Analysis for the Infected, Pre-AIDS and AIDS Patient of the HIV/AIDS Model

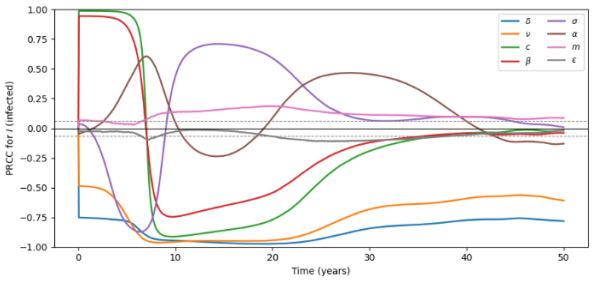

(a) PRCC trend over time–Infected Human

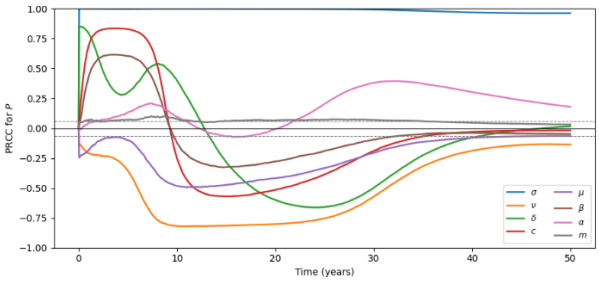

(b) PRCC trend over time–Pre-AIDS Patient

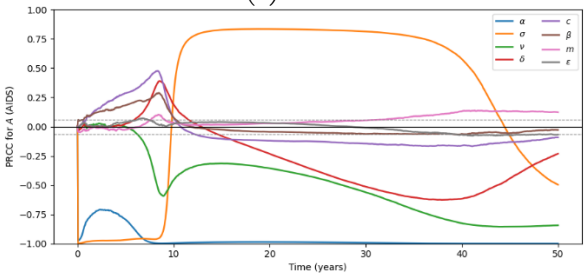

(c) PRCC trend over time–AIDS Patient

Figure 5: PRCC trend for the Infected Human/Mosquitoes of the Malaria Model

For the infected population (I), the natural mortality rate ν, progression rate δ, number of partners per individual c, and sexual contact rate β are the dominant drivers, alongside σ. Their signs, however, are time-dependent: early in the epidemic β and c are strongly positive (higher transmission accelerates infection), but past the epidemic peak they turn negative, as faster transmission depletes the susceptible pool and lowers later prevalence, while ν and δ remain persistently negative throughout. For the pre-AIDS class (P), σ is the overwhelmingly dominant positive driver, followed by ν (-) and μ (-), (representing exit from the compartment) and δ (+), consistent with σ and δ governing inflow to P and μ, ν governing outflow. For AIDS

cases (A), the AIDS-related disease-induced death rate α is the strongest negative influence and ν the second, confirming that progression-out rates control the AIDS burden. σ and δ contribute moderate positive effects, and the transmission parameters are only weakly influential, their effect on A is indirect, mediated through I and P.

Data-Driven Approach: Malaria

Here, we consider a model to understand the transmission dynamics of malaria developed in Rajnarayanan and Kumar (2024). As malaria involves two interacting species, the model considers both the human and mosquito populations. The human population is divided into three compartments; Susceptible, Infected and Recovered (SIR), while the mosquitoes' population is divided into two compartments; Susceptible and Infected (SI). The overall framework used in this study is the $SIR-SI$ model. The susceptible humans S_h) decreases over time when they come in contact with infected mosquitoes (I_m), leading to an increase in the infected population (I_h). The infected human population decreases as individuals recovers from malaria and move to the recovered class (R_h). Similarly, the number of susceptible mosquitoes (S_m) decreases over time as the infected humans come in contact with them, which leads to an increase in the population of the infected mosquito population.

The system of ODEs describing the dynamics of the spread of malaria is given by

$$\begin{aligned}
\frac{dS_h}{dt} &= \Gamma_h N_h - \frac{\beta_h}{N_h} S_h I_m - \mu_h S_h \\
\frac{dI_h}{dt} &= \frac{\beta_h}{N_h} S_h I_m - \gamma_h I_h - \mu_h I_h \\
\frac{dR_h}{dt} &= \gamma_h I_h - \mu_h R_h \qquad (15) \\
\frac{dS_m}{dt} &= \Gamma_m N_m - \frac{\beta_m}{N_m} S_m I_h - \mu_m S_m \\
\frac{dI_m}{dt} &= \frac{\beta_m}{N_m} S_m I_h - \mu_m I_m
\end{aligned}$$

Table 3 describes the parameters used in the $SIR-SI$ model and Figure 6 illustrate the interaction between the various compartments.

Table 3: Description of the parameters of the malaria model

Parameter	Description
Γ_h	Birth rate of humans
β_h	Transmission rate of malaria in humans
μ_h	Mortality rate of humans due to malaria
γ_h	Recovery rate of humans
Γ_m	Birth rate of mosquitoes
β_m	Transmission rate of malaria in mosquitoes
μ_m	Mortality rate of mosquitoes
N_h	Total human population: $N_h = S_h + I_h + R_h$
N_m	Total mosquito population: $N_m = S_m + I_m$

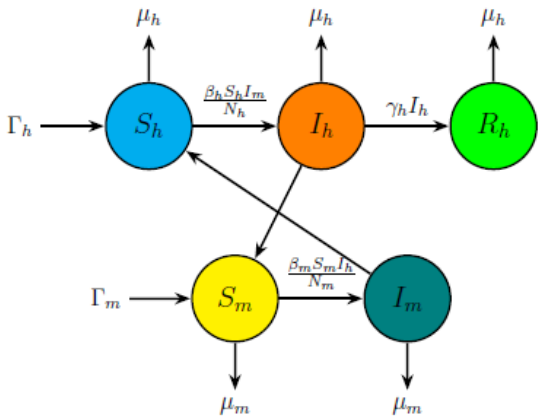

Figure 6: Flow Diagram of the Malaria model

For the simulation of model (15), we used a real-world data on the monthly incidence of malaria in Benue State collected from the Benue State Ministry of Health (Adeniyi et al., 2023). The dataset covers a 40-months period (from June 2013 to September 2016), and includes monthly values for infected humans, infected mosquitoes, recovered humans, susceptible humans and susceptible mosquitoes.

Data Processing of the Malaria Data

The raw dataset consists of 40 monthly observations for five epidemiological compartments: S_h, I_h, R_h (susceptible, infected, and recovered humans) and S_m, I_m (susceptible and infected mosquitoes). The neural network requires computing time derivatives via automatic differentiation, which in turn requires dense, smooth data; 40 monthly points are far too sparse for this purpose.

Method. Month index k is mapped to day $k \times 30$, then a *scipy.interpolate.CubicSpline* is fitted through all 40 knots, producing 1171 daily points spanning days 0 – 1170. The spline passes exactly through every monthly observation by construction. A *np.clip(..., 0)* removes the small negative undershoots that cubic splines can introduce between knots.

Table 4: Data Split

Train	70%	819 daily points
Validation	15%	176 daily points
Test	15%	176 daily points

Layers of the Architecture

The neural network designed for the $SIR-SI$ model consists of 8 fully connected hidden layers, each containing 32 neurons.

Table 5: The Components of the Neural Network Architecture

Component	Specification
Input Layer	Time
Hidden Layer	8 layers × 32 units, tanh activation
Output Layer	5 values — one per compartment $[S_h, I_h, R_h, S_m, I_m]$

The number of neurons were increased to 32 units, which aids the model to converge more slowly, giving the physics loss time to shape the learned dynamics; the best validation epoch occurs around epoch 10,000. The network is trained to produce values in [0, 1] because the targets are *min max normalized* to that range; the MSE loss drives the outputs there without an explicit constraint.

Training Procedure

- **Optimizer**
  Adam with $\eta = 10^{-3}$, weight_decay = 5×10^{-4} (L2 regularisation). Weight decay

acts as an additional overfitting brake on top of the architectural constraints.

- **Learning Rate Scheduler**
  ReduceLROnPlateau(mode='min', factor=0.5, patience=1000, min_lr=1e-6). Every time the validation loss fails to improve for 1000 consecutive epochs, the learning rate is halved. This allows fine-grained improvement in the late training phase (epochs 6k–15k) without oscillations.

- **Early Stopping**
  Best validation loss is tracked with patience = 5000 and $\delta_{min} = 10^{-7}$. If the validation loss does not improve by more than δ_{min} for 5000 consecutive epochs, training stops and the best weights are restored. Training reached epoch 15646 (best validation at epoch ≈10646).

Transient Val Loss Increase at Epoch ≈11 000
The Val loss briefly rises to 0.049 at epoch 11000 before returning to 0.041 at epoch 12000. The epoch log shows Γ_h growing from 0.01 (epoch 6000) to 0.51 (epoch 11000) to 0.88 (epoch 15000). Γ_h and μ_h must remain near equal to preserve S_h conservation, and a brief mismatch during rapid growth causes transient ODE instability. This is a fundamental consequence of the *softplus parameterisation:* the optimizer discovers the near conservation constraint gradually.

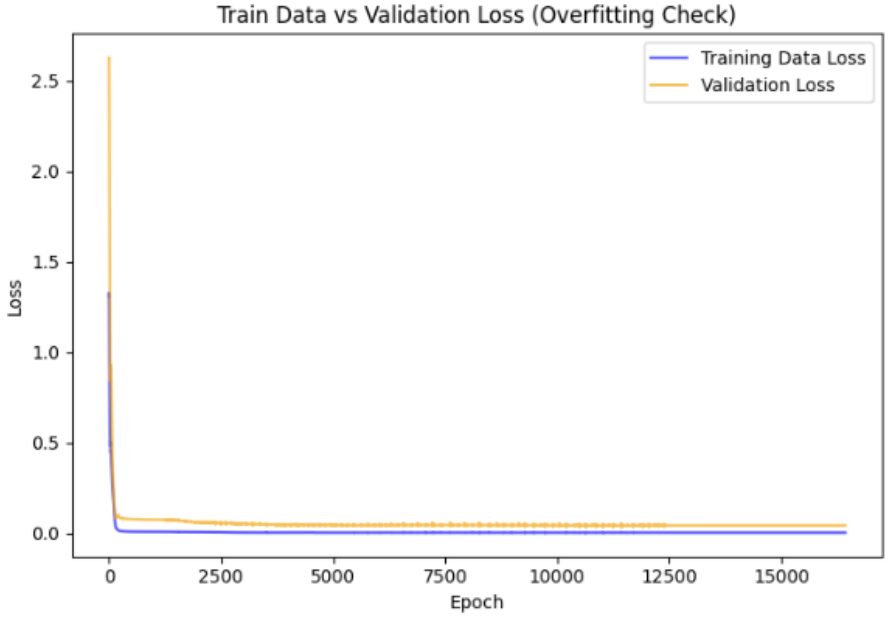

Figure 7: The Loss for the Train data and the Validation Loss

The relative root mean square error for the five compartments of the malaria model over time are as follows:

Table 6: Relative root Mean Square Error (RMSE) for the five compartment of the Malaria Model

Split	S_h	I_h	R_h	S_m	I_m
Train	0.00058	0.04265	0.04685	0.00066	0.00071
Val	0.00651	0.12427	0.13105	0.00660	0.00656
Test	0.01406	0.34954	0.34469	0.01598	0.01590

Monotone compartments (S_h, S_m, I_m) generalise very well: *val/test RMSE <2%.* Oscillating compartments (I_h, R_h) are excellent in training (≈4–5%), acceptable in validation (≈13%), and poor in test (≈35%) — the test degradation arises from amplitude drift, not from a failure to learn the seasonal pattern.

The trained neural network estimates the learnable parameters Γ_h, β_h, μ_h, γ_h, Γ_m, β_m, and μ_m. Table 7 summarizes the estimated parameter values, while Figure 8 presents a visual comparison between actual and predicted outcomes.

Table 7: Parameter Estimation – Malaria

Parameters	Range	Estimated Parameter
Γ_h	(-1, 1)	0.624461 (per-day)
β_h	(-1, 1)	0.48613 (per-day)
μ_h	(-1, 1)	0.601185 (per-day)
γ_h	(-1, 1)	0.696181 (per-day)
Γ_m	(-1, 1)	0.212516 (per-day)
β_m	(-1, 1)	0.53702 (per-day)
μ_m	(-1, 1)	0.201283 (per-day)

For the malaria model, we increased the number of training epochs, which consequently resulted in a longer training time for the neural network. From the results obtained, it can be observed that the longer the training time, the better the performance of the network training. All other parameters including the learning rate, number of hidden layers, number of neurons, and range of parameters, were kept constant. However, they can be adjusted to improve the performance.

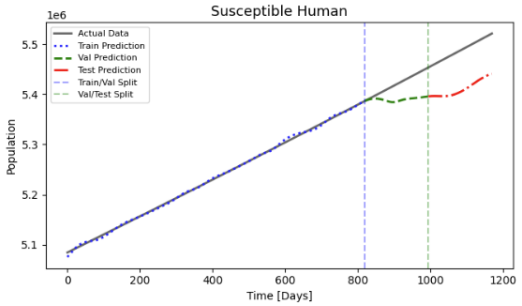

(a) Actual vs Predicted Susceptible Humans

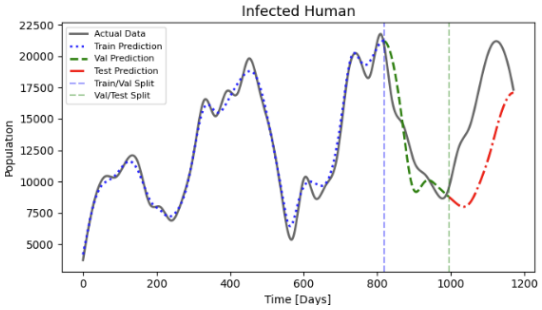

(b) Actual vs Predicted Infected Humans

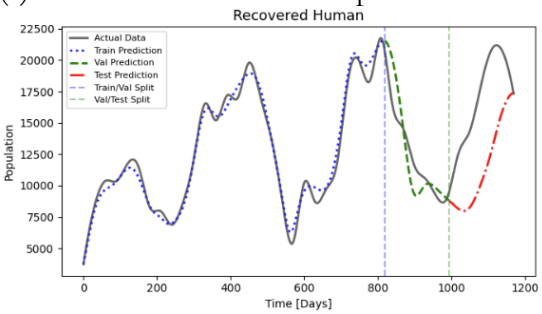

(c) Actual vs Predicted Recovered Humans

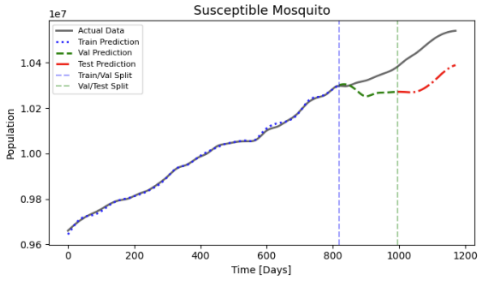

(d) Actual vs Predicted Susceptible Mosquitoes

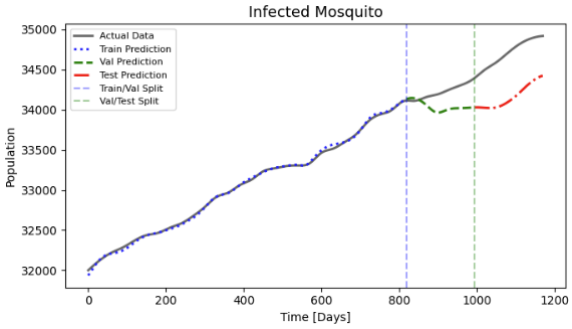

(e) Actual vs Predicted Infected Mosquitoes

Figure 8: Actual vs Predicted Compartments of the Malaria model

Global Sensitivity Analysis (PRCC)

A global sensitivity analysis was performed using Latin Hypercube Sampling with partial rank correlation coefficients (PRCC), computed over time for the infected human (I_h) and infected mosquito (I_m) compartments. Figure 9 reports the PRCC at day 1170, and Figure 10 shows how each parameter's influence evolves over the transmission season.

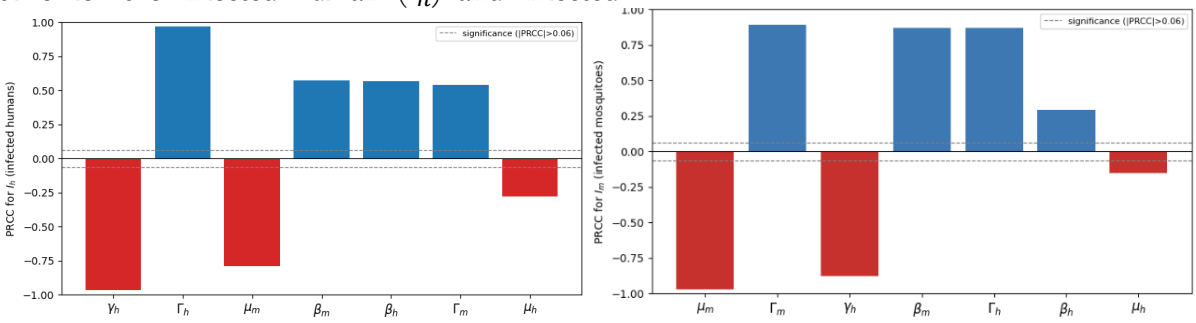

(a) PRCC at day 1170 – Infected Human (b) PRCC at day 1170– Infected Mosquitoes

Figure 9: Sensitivity Analysis for the Infected Human/Mosquitoes of the Malaria Model

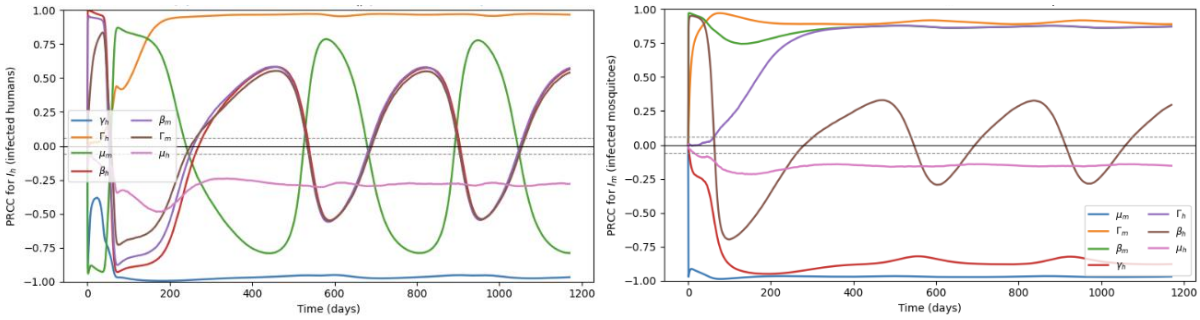

(a) PRCC trend over time–Infected Human (b) PRCC trend over time–Infected Mosquitoes

Figure 10: PRCC trend for the Infected Human/Mosquitoes of the Malaria Model

For infected humans (I_h), the human birth rate Γ_h is the strongest positive driver, while the recovery rate γ_h is the strongest negative one, which shows that expanding the susceptible pool raises infection, and faster recovery suppresses it. The mosquito mortality rate μ_m is a powerful negative influence, confirming vector control as the most effective lever, and the transmission rates β_h, β_m together with mosquito recruitment Γ_m contribute moderate positive effects. Human mortality μ_h is weakly influential. For infected mosquitoes (I_m), μ_m dominates negatively, followed by mosquito recruitment Γ_m (+), human recovery γ_h (−), and transmission β_m (+), while β_h and μ_h are comparatively minor.

Benchmarking Against Classical and Data-Driven Models

We compared the Neural ODE against a classical RK4 and a data-driven LSTM on the malaria dataset, employing same temporal split using relative RMSE metric. The comparison reveals a compartment-dependent trade-off rather than uniform superiority: the Neural ODE achieves the lowest training and validation error overall and the smallest test error on the smooth compartments (S_h, S_m, I_m), while the classical RK4 model retains an advantage on the sharply oscillatory human compartments (I_h, R_h) under long-range extrapolation, with the LSTM falling between the two. Table 8 reports the relative RMSE for each compartment across the training, validation, and test sets, while Figure 11 visualizes these errors and makes the compartment-dependent trade-off between the models apparent.

Table 8: RMSE for each compartment using Neural ODEs, RK4 and LSTM

Model	Split	S_h	I_h	R_h	S_m	I_m
Neural ODE	Train	0.0005	0.0360	0.0373	0.0005	0.0006
RK	Train	0.0192	0.1236	0.1230	0.0183	0.0556
LSTM	Train	0.0021	0.0675	0.0666	0.0022	0.0021
Neural ODE	Val	0.0068	0.1325	0.1374	0.0069	0.0069
RK4	Val	0.0417	0.0783	0.0898	0.0396	0.0517
LSTM	Val	0.0151	0.2024	0.1901	0.0144	0.0151
Neural ODE	Test	0.0140	0.3060	0.3046	0.0158	0.0157
RK4	Test	0.0551	0.0566	0.0961	0.0528	0.1422
LSTM	Test	0.0250	0.1845	0.2013	0.0241	0.0246

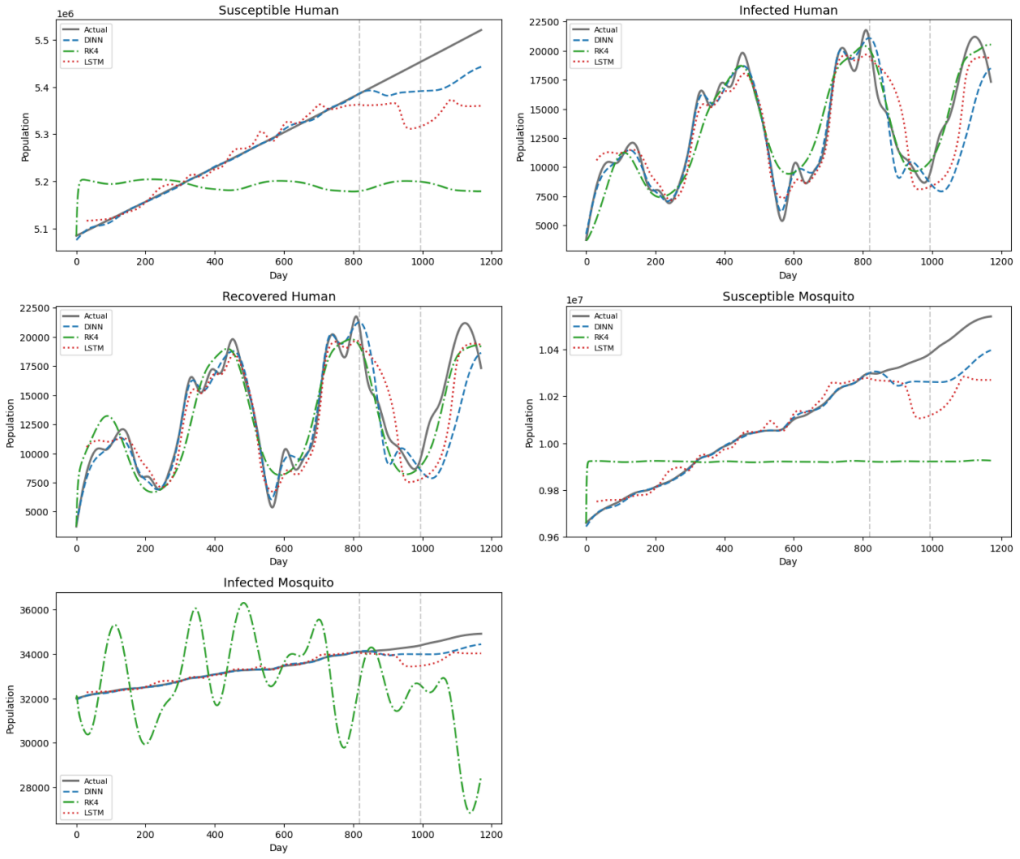

Figure 11: Comparison between the Neural ODEs, RK4 and LSTM model

Future Predictions for Diseases with Real-Life Data

Following the simulation and validation of the HIV/AIDS and malaria models, the trained Neural ODE frameworks were employed to generate future projections for both diseases.

The trained Neural ODE model based on the SIR-SI compartmental model was also employed to forecast the transmission dynamics of malaria over the next 10 months. The model was trained with a learning rate of 1×10^{-9} for 300,000 epochs requiring approximately 50 mins 5 secs. Figure 6 presents the predicted evolution of all compartments with the malaria model for both human and mosquito population.

These projections demonstrate the capability of the Neural ODE approach not only to fit historical epidemiological data but also to provide meaningful short- to medium-term forecasts for infectious disease.

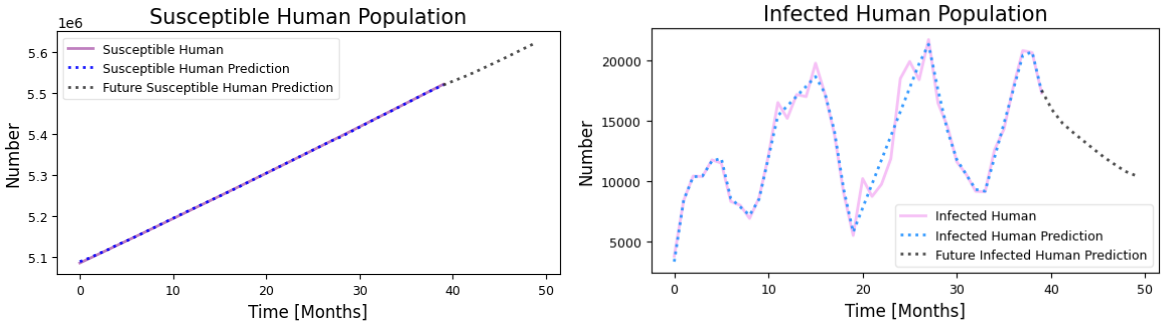

(a)Future Prediction of the Susceptible human (b) Future Prediction of the Infected human

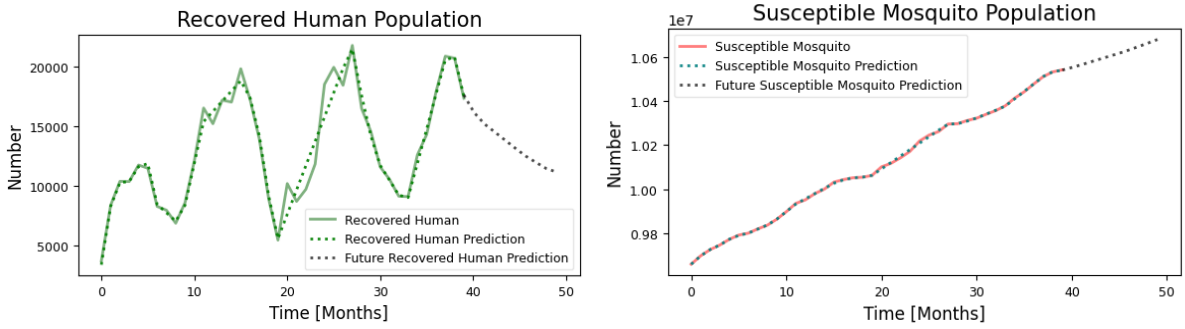

(c) Future Prediction Recovered Human (d) Future Prediction of Susceptible Mosquito

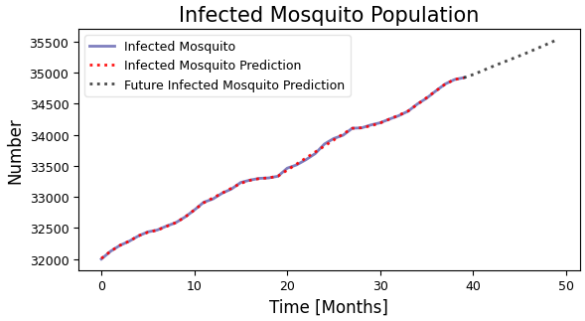

(e) Future Prediction of the Infected Mosquito

Figure 10: Future spread of each compartment of the Malaria model

CONCLUSION

This study has demonstrated the effectiveness of Neural Ordinary Differential Equations (Neural ODEs) in modelling, parameter estimation, and forecasting the transmission dynamics of selected diseases. By integrating classical compartmental epidemiological models with disease-informed neural networks, the proposed framework successfully combined mechanistic understanding with data-driven learning.

The results show that the Neural ODE approach accurately captures the temporal evolution of disease compartments and reliably estimates key epidemiological parameters without prior specification. The model performed effectively for both real-world datasets (malaria) and synthetically generated datasets (HIV/AIDS), demonstrating its flexibility and robustness across different disease structures. Increased training epochs were found to enhance predictive accuracy, enabling the model to better represent complex nonlinear transmission patterns.

Despite these promising outcomes, the study highlights a trade-off between predictive performance and computational cost, as longer training durations were required for improved accuracy. Future research may therefore focus on improving computational efficiency, incorporating additional epidemiological factors such as demographic heterogeneity and intervention strategies, and extending the framework to other

infectious diseases or real-time surveillance systems.

Overall, the Neural ODE framework provides a powerful and adaptable tool for epidemiological modelling, parameter inference, and disease forecasting, with potential applications in public health planning and decision-making.

Further research will focus on integrating adaptive Runge-Kutta methods into Neural ODE frameworks to capture stiff dynamics within the system and comparing this approach to other Neural ODE models in the literature. Furthermore, a statistical property of the predictions and errors to determine uncertainty will be investigated.

ACKNOWLEDGEMENTS

The authors would like to thank the anonymous reviewers for their valuable comments and suggestions which has improved the quality of this paper. The authors are grateful to the University of Lagos, Akoka for making available the computer laboratory at the central research laboratory for the simulation of this research.

FUNDING STATEMENT

This research was supported by the 2024 University of Lagos Central Research Committee (CRC) under grant CRC-2025/11, 2024 Tertiary Education Task Fund (TETFUND) National Research Fund (NRF) under grant TETF/ES/DR\&D-CE/NRF2024/CC/EHU/00072 and partially supported by a grant from the IMU, supported by the Friends of IMU (FIMU), under the IMU Breakout Fellowship Program. The funders had no role or influence on the design and interpretation of the data collected, as well as in writing the manuscript.

CONFLICT OF INTEREST The authors declare no conflict of interest.

AUTHORS' CONTRIBUTIONS

The study was conceived and designed by J.O.E, F.C.N and S.A.O; Data collection was coordinated by F.C.N, J.O.E. and S.A.O.; F.C.N. and J.O.E. conducted the data analysis and software design; F.C.N. prepared the first draft of the manuscript; F.C.N., J.O.E. and S.A.O. reviewed and edited the manuscript. J.O.E. and S.A.O. supervised the research. All authors read and approved the final manuscript.

REFERENCES

Adeniyi, M. O., Aderele, O. R., Oludoun, O. Y., Ekum, M. I., Matadi, M. B., Oke, S. I., & Ntiamoah, D. (2023). A mathematical and exploratory data analysis of malaria disease transmission through blood transfusion. *Frontiers in Applied Mathematics and Statistics*, *9*, 1105543. doi: 10.3389/fams.2023.1105543

Aron, J. L., & Schwartz, I. B. (1984). Seasonality and period-doubling bifurcations in an epidemic model. *Journal of theoretical biology*, *110*(4), 665-679. doi: 10.1016/S0022-5193(84)80150-2

Asri, M., Sidjara, S., Sanusi, W., Side, S., & Pratama, M. I. (2021). Analysis and solution of the SEIRS model for the Rubella transmission with vaccination effect using Runge-Kutta method. In *Journal of Physics: Conference Series* (Vol. 1899, No. 1, p. 012090). IOP Publishing. doi: 10.1088/1742-6596/1899/1/012090

Chen, R. T., Rubanova, Y., Bettencourt, J., & Duvenaud, D. K. (2018). Neural ordinary differential equations. *Advances in neural information processing systems*, 31.

Choisy, M., Guégan, J. F., & Rohani, P. (2007). Mathematical modeling of infectious diseases dynamics. *Encyclopedia of infectious diseases: modern methodologies*, 379. doi: 10.25334/0G39-8F29

Han, S., Stelz, L., Stoecker, H., Wang, L., & Zhou, K. (2024). Approaching epidemiological dynamics of COVID-19 with physics-informed neural networks. *Journal of the Franklin Institute*, *361*(6), 106671. doi: 10.1016/j.jfranklin.2024.106671

Kamina, K. M., Mwalili, S., & Wanjoya, A. (2019). The modeling of a stochastic SIR model for HIV/AIDS epidemic using Gillespie's algorithm. *Int. J. Data Sci. Anal*, *5*(6), 117. doi: 10.11648/j.ijdsa.20190506.12

Kermack, W. O., & McKendrick, A. G. (1927). A contribution to the mathematical theory of epidemics. *Proceedings of the Royal Society of London. Series A, Containing papers of a mathematical and physical character*, *115*(772), 700-721. doi: 10.1098/rspa.1927.0118

Kibona, I. (2011). A deterministic model of HIV/AIDS with vertical transmission in the presence of infected immigrants. *International Journal of Physical Sciences*. 6(23), 5383 – 5398. doi: 10.5897/IJPS11.452

Kosma, C., Nikolentzos, G., Panagopoulos, G., Steyaert, J. M., & Vazirgiannis, M. (2023). Neural ordinary differential equations for modeling epidemic spreading. *Transactions on Machine Learning Research*.

Liu, Z., Wan, G., Prakash, B. A., Lau, M. S., & Jin, W. (2024, August). A review of graph neural networks in epidemic modeling. In *Proceedings of the 30th ACM SIGKDD conference on knowledge discovery and data mining* (pp. 6577-6587). doi: 10.1145/3637528.3671455

Mandal, S., Sarkar, R. R., & Sinha, S. (2011). Mathematical models of malaria-a review. *Malaria journal*. *10*(1), 202. doi: 10.1186/1475-2875-10-202.

Millevoi, C., Pasetto, D., & Ferronato, M. (2024). A Physics-Informed Neural Network approach for compartmental epidemiological models. *PLOS Computational Biology*, *20*(9), e1012387. doi: 10.1371/journal.pcbi.1012387

Rajnarayanan, A., Kumar, M., & Tridane, A. (2025). Analysis of a mathematical model for malaria using data-driven approach. *Scientific reports*, *15*(1), 27272. doi: 10.1038/s41598-025-12078-4

Rodríguez, A., Cui, J., Ramakrishnan, N., Adhikari, B., & Prakash, B. A. (2023). Einns: epidemiologically-informed neural networks. In *Proceedings of the AAAI conference on artificial intelligence*. 37(12), 14453-14460. doi: 10.1609/aaai.v37i12.26690

Shaier, S., Raissi, M., & Seshaiyer, P. (2021). Data-driven approaches for predicting spread of infectious diseases through DINNs: Disease Informed Neural Networks. *arXiv preprint arXiv:2110.05445*.

Sharma, A., Kumar, A., Dhanka, S., Maini, S., Rautela, K., Kant, S., ... & Palta, A. (2026). Artificial Intelligence in Epidemic Modeling and Pandemic Preparedness: A Comprehensive Review. *Archives of Computational Methods in Engineering*, 33, 7085 – 7115. doi: 10.1007/s11831-026-10525-7.

Simangunsong, L., & Mungkasi, S. (2021). Fourth order Runge-Kutta method for solving a mathematical model of the spread of HIV-AIDS. In *AIP Conference Proceedings* (Vol. 2353, No. 1, p. 030092). AIP Publishing LLC. doi: org/10.1063/5.0052550

Turner, A., Jung, C., Tan, P., Gotika, S., & Mago, V. (2015). A comprehensive model of spread of malaria in humans and mosquitos. In *SoutheastCon 2015* (pp. 1-6). IEEE. doi: 10.1109/SECON.2015.7132968

Wan, G., Liu, Z., Lau, M. S., Prakash, B. A., & Jin, W. (2024). Epidemiology-aware neural ode with continuous disease transmission graph. *arXiv preprint arXiv:2410.00049*.

Wang, Z., Wang, Q., & Klinke, D. J. (2016). Simulation study on effects of order and step size of Runge-Kutta methods that solve contagious disease and tumor models. *Journal of computer science and systems biology*, *9*(5), 163 – 172. doi: 10.4172/jcsb.1000234

Yion, C. (2023). SIR integrated model based on Runge-Kutta for Polio Vaccination Analysis. *Journal of Quality Measurement and Analysis JQMA*, *19*(1), 1-11.

Zakary, O., Rachik, M., & Elmouki, I. (2016). On the impact of awareness programs in HIV/AIDS prevention: an SIR model with optimal control. *Int. J. Comput. Appl*, *133*(9), 1-6.